SINTEF
PROCEEDINGS
2

Proceedings of the 12th International Conference on Computational Fluid Dynamics in the Oil & Gas, Metallurgical and Process Industries

Progress in Applied CFD – CFD2017

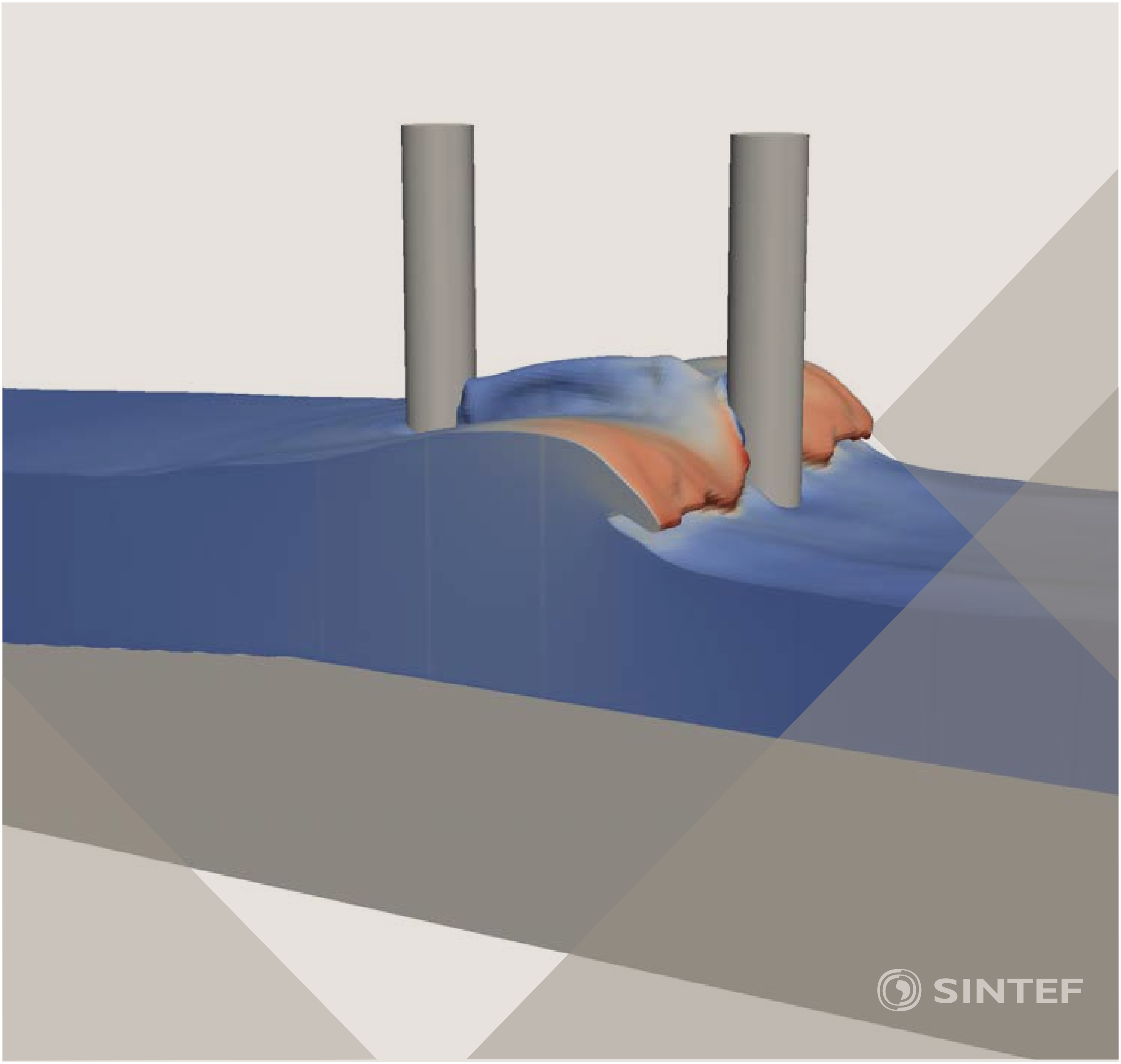

SINTEF Proceedings

Editors:
Jan Erik Olsen and Stein Tore Johansen

Progress in Applied CFD – CFD2017

Proceedings of the 12th International Conference on Computational Fluid Dynamics in the Oil & Gas, Metallurgical and Process Industries

SINTEF Academic Press

SINTEF Proceedings no 2
Editors: Jan Erik Olsen and Stein Tore Johansen
Progress in Applied CFD – CFD2017
Selected papers from 10th International Conference on Computational Fluid Dynamics in the Oil & Gas, Metallurgical and Process Industries

Key words:
CFD, Flow, Modelling

Cover, illustration: Arun Kamath

ISSN 2387-4295 (online)
ISBN 978-82-536-1544-8 (pdf)

SINTEF Academic Press

Address:	Forskningsveien 3 B
	PO Box 124 Blindern
	N-0314 OSLO
Tel:	+47 73 59 30 00
Fax:	+47 22 96 55 08

www.sintef.no/byggforsk
www.sintefbok.no

SINTEF Proceedings
SINTEF Proceedings is a serial publication for peer-reviewed conference proceedings on a variety of scientific topics.
The processes of peer-reviewing of papers published in SINTEF Proceedings are administered by the conference organizers and proceedings editors. Detailed procedures will vary according to custom and practice in each scientific community.

PREFACE

This book contains all manuscripts approved by the reviewers and the organizing committee of the 12th International Conference on Computational Fluid Dynamics in the Oil & Gas, Metallurgical and Process Industries. The conference was hosted by SINTEF in Trondheim in May/June 2017 and is also known as CFD2017 for short. The conference series was initiated by CSIRO and Phil Schwarz in 1997. So far the conference has been alternating between CSIRO in Melbourne and SINTEF in Trondheim. The conferences focuses on the application of CFD in the oil and gas industries, metal production, mineral processing, power generation, chemicals and other process industries. In addition pragmatic modelling concepts and bio-mechanical applications have become an important part of the conference. The papers in this book demonstrate the current progress in applied CFD.

The conference papers undergo a review process involving two experts. Only papers accepted by the reviewers are included in the proceedings. 108 contributions were presented at the conference together with six keynote presentations. A majority of these contributions are presented by their manuscript in this collection (a few were granted to present without an accompanying manuscript).

The organizing committee would like to thank everyone who has helped with review of manuscripts, all those who helped to promote the conference and all authors who have submitted scientific contributions. We are also grateful for the support from the conference sponsors: ANSYS, SFI Metal Production and NanoSim.

Stein Tore Johansen & Jan Erik Olsen

Organizing committee:

Conference chairman: Prof. Stein Tore Johansen
Conference coordinator: Dr. Jan Erik Olsen
Dr. Bernhard Müller
Dr.Sigrid Karstad Dahl
Dr.Shahriar Amini
Dr.Ernst Meese
Dr.Josip Zoric
Dr.Jannike Solsvik
Dr.Peter Witt

Scientific committee:

Stein Tore Johansen, SINTEF/NTNU
Bernhard Müller, NTNU
Phil Schwarz, CSIRO
Akio Tomiyama, Kobe University
Hans Kuipers, Eindhoven University of Technology
Jinghai Li, Chinese Academy of Science
Markus Braun, Ansys
Simon Lo, CD-adapco
Patrick Segers, Universiteit Gent
Jiyuan Tu, RMIT
Jos Derksen, University of Aberdeen
Dmitry Eskin, Schlumberger-Doll Research
Pär Jönsson, KTH
Stefan Pirker, Johannes Kepler University
Josip Zoric, SINTEF

CONTENTS

FLOW PAST A YAWED CYLINDER OF FINITE LENGTH USING A FICTITIOUS DOMAIN METHOD

Jean-Lou PIERSON[1]*, Abdelkader HAMMOUTI[1], Franck AUGUSTE[2], Anthony WACHS[3]

[1]IFP Energies nouvelles, 69360 Solaize, France

[2]UMR5318-CECI, CERFACS/CNRS, Toulouse, France & IMFT, Allee du Professeur Camille Soula, 31400 Toulouse

[3]Department of Mathematics, University of British Columbia, 1984 Mathematics Road, Vancouver, BC, Canada V6T 1Z2, Department of Chemical & Biological Engineering, University of British Columbia, 2360 East Mall, Vancouver, BC, Canada V6T 1Z3

* E-mail: jean-lou.pierson@ifpen.fr

ABSTRACT

In this work, the flow past a finite-end yawed cylinder is studied. This constitute a first step to understand the motion of freely moving particles. To this aim the Finite Volume / Fictitious Domain (FV/FD) method developed in the PeliGRIFF code (Wachs *et al.*, 2015) is intensively used. This method is validated using numerical results of the literature for a cylinder of finite length whose direction is parallel to the flow (Auguste, 2010). Efforts and vortex shedding frequencies are carefully analysed giving strong confidence in the numerical methodology. A detail study of the flow past a cylinder of aspect ratio $L/D = 3$ (where D is the diameter and L the length) at moderate Reynolds numbers ($Re = \rho UD/\mu = 200$) is also carried out. The influence of the yaw angle (ranging from 0° to 90°) is identified both on the wake and on the hydrodynamic efforts. Three different regimes are successively encountered including standing-eddy pattern as unsteady vortex shedding. Otherwise the independence principle which states that the normal force on the cylinder only depends on the normal component of the velocity (Sears, 1948), is compared to the numerical simulations. Results indicate that the independence principle is inaccurate in this flow regime. A linear law obtained in the Stokes regime should be preferred.

Keywords: Fictitious domain method, finite-end cylinder, hydrodynamic forces, wake instability .

INTRODUCTION

Fixed and fluidized beds are frequently encountered in various industrial processes such as catalyse and biomass gasification. Despite the large numbers of studies describing the flow past spherical particles, much less is known concerning cylindrical particles which are frequently used in fixed and bubbling fluidised bed. In order to fill that gap direct numerical simulation have been used to study the flow through a packed bed of cylinders. For instance (Dorai *et al.*, 2015) highlight the impact of the particle shape on the pressure drop through the bed. For computational reasons, Euler-Lagrange methods are usually preferred to direct numerical simulation to deal with a large number of fluidized particles. Those methods have been applied with success for spouted bed configurations and bubbling fluidized bed of spherical particles (Capecelatro and Desjardins, 2013; Bernard *et al.*, 2016). However the averaging procedure used to derive the Euler-Lagrange equations brings out more unknown than equations (Jackson, 2000). Closure law and especially hydrodynamic force exerted on the body are thus needed to solve the problem. To this aim the flow past a finite-length yawed cylinder is studied numerically as a first step to understand the efforts acting on many of them.

One of the earliest study of the flow past a cylinder oriented perpendicularly to the streamwise direction is the one of Wieselsberger (1922). Both infinite and two free ends cylinder were considered. For the former the aspect ratio L/D was 5, where L is the length of the cylinder and D its diameter. He covered a large range of Reynolds numbers $Re = \rho DU/\mu$ from 400 to 8×10^5 where μ, ρ and U are respectively the dynamic viscosity, density and inlet velocity. The drag coefficient was found to decrease when decreasing L/D. Zdravkovich *et al.* (1989) studied the flow past a perpendicular cylinder of finite aspect ratio ($1 \leq L/D \leq 10$) at high Reynolds numbers ($6 \times 10^4 \leq Re \leq 2.6 \times 10^5$). The drag coefficient was also observed to decrease when decreasing L/D. He observed a kind of vortex shedding in the range $2 \leq L/D \leq 8$ and an asymmetric flow pattern for $1 \leq L/D \leq 3$. Inoue and Sakuragi (2008) performed a detailed numerical study of the flow past finite length cylinder. The prescribed L/D and Reynolds number were respectively $0.5 \leq L/D \leq 100$ and $40 \leq Re \leq 300$. They identify five different vortex shedding patterns depending on both aspect ratio and Reynolds number. They also showed that the critical Reynolds number, for the onset of the unsteady regime, decreased with L/D.

Studies of the flow past yawed or aligned cylinders (whose symmetry axis is parallel to the incoming flow) are more sparse comparatively to the large amount of works on perpendicular cylinder. Auguste (2010) and Auguste *et al.* (2010) numerically studied the wakes of disks ($0 \leq L/D \leq 1$) parallel to the flow direction. The Reynolds number prescribed was $0 \leq Re \leq 400$. Auguste (2010) observed that the critical Reynolds for appearance of unsteady regime as the wake patterns are strongly varying function of the aspect ratio. To the author knowledge the bifurcation scenario for $L/D > 1$ have not been studied so far. Recently Chrust *et al.* (2010) evidenced the effect of L/D over the wake of spheroids parallel to the flow direction. Ramberg (1983) studied experimentally the flow past free-ended yawed cylinders and yawed cylinders fitted with end-plates in the Reynolds number range $160 \leq Re \leq 1100$. Cylinders were oriented to the flow direction at an angle θ. He showed that the results were very sensitive to the cylinder end conditions. Sears (1948) has theoretically demonstrated, using boundary layer theory, that the flow past a yawed cylinder is determinated by the normal component of the velocity. In other word the force on cylinder with a yawed angles θ was identical to the force on a cylinder in cross-flow with velocity $U \sin\theta$. This law called independence principle has been widely used to predict the force on a yawed cylinder. However this principle suffers from some limitation summarized in Zdravkovich (2003, p 955). Recently Vakil and Green (2009) performed a complete numerical analysis of the flow past a yawed cylinder ($2 \leq L/D \leq 20$) for moderate Reynolds number ($1 \leq Re \leq 40$). They proposed an empirical relation for the drag and lift force on the cylinder. They also checked the validity of the independence principle. Even if the range of Reynolds number studied was lower than the one for strict application of boundary layer theory they obtain relatively good agreement for large $\theta > 45°$.

Thus there is a large amount of works especially on the flow past perpendicular cylinder. An exhaustive review can be found in the two monographs of Zdravkovich (1997, 2003). A large part of the numerical study dealing with that subject make use of boundary-fitted method to describe the flow around the particle (Auguste, 2010; Inoue and Sakuragi, 2008; Vakil and Green, 2009). Those methods are very accurate but not designed to deal with a large number of mobile particles since they need re-meshing at each time steps (Hu *et al.*, 1992). For this kind of applications fictitious domain method are usually preferred. Indeed the boundary conditions on the particle are defined on the eulerian grid using forcing terms added to the governing equations (Mittal and Iaccarino, 2005). Those methods have been used and validated for the settling of spheroidal particles (Uhlmann and Dušek, 2014; Ardekani *et al.*, 2016). To the authors knowledge, analysis of the flow past a yawed cylinder using a fictitious domain method have not been done so far. Therefore before studying the flow past a yawed cylinder in inertial regimes, we will carefully validate our numerical method with existing results of the literature.

The outline of the paper is the following. In the first section the numerical method, flow geometry and boundary conditions are described. In the second section the flow past a yawed cylinder is studied. The first part of the second section is devoted to the comparison of our numerical results to those of the literature. The second part describes the flow past a $L/D = 3$ cylinder at $Re = 200$ for various yawed angles. Mains conclusions and future work are presented in the last section.

NUMERICAL PROCEDURES

Computations are carried out using the fictitious domain method of the PeliGRIFF code. A set of Lagrange points are distributed throughout the body in order to enforce the boundary conditions. In the rest of the section we summarize the principal features of the fictitious domain method developed by Wachs *et al.* (2015).

Time discretization scheme

The three dimensional unsteady incompressible Navier-Stokes equations are solved using a second-order time accurate Adams-Bashforth / Crank-Nicolson scheme. However due to a first-order Marchuk-Yanenko time splitting strategy the overall time algorithm is first-order accurate. Incompressibility is enforced at the end of the fluid time step through a projection method. The linear systems obtained from both Cranck-Nicolson and projection step are solved using PETSC library.

The overall time advancement procedure is described in the following.

- At the beginning of the time step the velocity of the fluid $\mathbf{u}^n$ and the pressure p^n are known. The n index refers to the time step.
- A mixed Adams-Bashforth / Crank-Nicolson scheme is employed to compute $\tilde{\mathbf{u}}^{n+1}$. Then a Poisson equation is solved to find a divergence free velocity $\hat{\mathbf{u}}^{n+1}$ and p^{n+1} :

$$\frac{\tilde{\mathbf{u}}^{n+1} - \mathbf{u}^n}{\Delta t} - \frac{1}{2}\frac{\mu}{\rho}\nabla^2\tilde{\mathbf{u}}^{n+1} = -\frac{1}{\rho}\nabla p^n + \frac{1}{2}\frac{\mu}{\rho}\nabla^2\mathbf{u}^n - \frac{1}{2}\left(3\mathbf{u}^n \cdot \nabla\mathbf{u}^n - \mathbf{u}^{n-1} \cdot \nabla\mathbf{u}^{n-1}\right) - \mathbf{f}^n, \quad (1a)$$

$$\nabla^2\psi^{n+1} = \frac{1}{\Delta t}\nabla \cdot \tilde{\mathbf{u}}^{n+1}, \quad (1b)$$

$$\hat{\mathbf{u}}^{n+1} = \tilde{\mathbf{u}}^{n+1} - \Delta t \nabla\psi^{n+1}, \quad (1c)$$

$$p^{n+1} = p^n + \psi^{n+1} - \frac{1}{2}\frac{\Delta t \mu}{\rho}\nabla^2\psi^{n+1} \quad (1d)$$

where ρ is the fluid density, μ the viscosity, ψ^n the auxiliary potential and $\mathbf{f}^n$ is the explicit forcing term used to take into account the presence of the rigid body.

- A fictitious domain problem which is solved using an Uzawa algorithm Wachs (2009). For a fixed body configuration the problem can be written such that $\mathbf{u}^{n+1}$ and $\mathbf{f}^{n+1}$ satisfy in the body region :

$$\frac{\mathbf{u}^{n+1} - \hat{\mathbf{u}}^{n+1}}{\Delta t} + \mathbf{f}^{n+1} = \mathbf{f}^n, \quad (2a)$$

$$\mathbf{u}^{n+1} = \mathbf{0} \quad (2b)$$

Unlike Uhlmann (2005); Bigot *et al.* (2014), the incompressibility condition is enforced before the imposition of boundary conditions on the particle. The main consequence is that the mass conservation is not exactly satisfied while the boundary conditions are exactly satisfied.

The hydrodynamic force and torque on the body can be written respectively $\mathbf{F} = \int_S \boldsymbol{\sigma} \cdot \mathbf{n} dS$ and $\mathbf{T} = \int_S \mathbf{r} \times \boldsymbol{\sigma} \cdot \mathbf{n} dS$ where $\boldsymbol{\sigma}$ is the stress tensor, $\mathbf{r}$ the the local position relative to the solid centroid and $\mathbf{n}$ the unit normal to the body surface S. The direct evaluation of these terms are complicated due to to the many interpolations required. An approach similar to the one proposed by Uhlmann (2005) was preferred. The surface integral of the hydrodynamic force and torque are replaced by $\rho \int_V \mathbf{f}^{n+1} dV$ and $\rho \int_V \mathbf{r} \times \mathbf{f}^{n+1} dV$ where V is the particle volume.

Space discretization scheme

Equations (1a)-(1d) are solved on a staggered cartesian grid with a finite volume approach. A second order central discretization scheme is employed for the diffusion term while the convective term is treated with a total variation diminishing (TVD) scheme and Superbee flux limiter. However due to the presence of the immersed boundary, the method is not fully second order in space (Wachs *et al.*, 2015).

In order to enforce the boundary conditions on the body, a set of lagrangian points are distributed along the surface and inside the particle. Interior points are distributed on the staggered grid at the same location that the velocity points. Distribute points uniformly along the particle surface is much more challenging. The detailed method developed in the PeliGRIFF code is described in a companion paper (Pierson *et al.*, 2017). The basic idea is to divide the cylinder in two main areas : its length and the two ending disks. The area defined along the length of the body can be mapped using a diamond-shaped mesh while the disks can be mapped with a specific spiral distribution. This methodology ensures that the points are uniformly and isotropically distributed. This property have been proved to be important for computation of the flow past a sphere (Wachs *et al.*, 2015).

The explicit forcing term in equation 1 is smoothed using a simple hat function of 3 cells length support. This simple procedure have proven to be efficient in all cases studied by the past (Wachs *et al.*, 2015; Rahmani and Wachs, 2014) and contain some similarities with the delta function used by Uhlmann (2005) and Kempe and Fröhlich (2012). While it would be possible to use the same type of delta function to interpolate the forcing term on the Lagrangian points, a quadratic interpolation operator was preferred (Wachs *et al.*, 2015). Indeed, since the construction of the 3D stencil of this operator relies on the orientation of the outward normal vector to the particle boundary, a good spatial accuracy can be achieved (Wachs *et al.*, 2015).

Computational domain

The building of a relevant numerical domain valid in all configurations studied (various aspect ratios and yawed angles) while keeping its size reasonable is a challenging task. To our knowledge there is no consensus in the literature on the size of the domain to used. In the following we briefly review several computational domains used by the past in the literature. The length and radius of the cylindrical domain used by Auguste (2010) are respectively $25D$ and $10D$ where D is the diameter of the disk. He focused on the flow past various disks of aspect ratio varying from zero to one. Special attention is paid to the distance between the disk and the outlet boundary condition which have to be at least of $15D$ to avoid errors on the computation of the hydrodynamic force. Inoue and Sakuragi (2008) studied the flow past cylinders directed perpendicular to the flow. In their study, the aspect ratio varied from 0.5 to 100. They defined five computational domain depending on the range of aspect ratio studied. In particular the length of the domains range from $115D$ to $190D$. The height of the domains, whose normal is parallel to the axis of the cylinder, vary linearly with L (as $L+60D$) while its depth is equal to $=60D$ and is thus fixed for all aspect ratio studied. Vakil and Green (2009) studied the flow past a yawed cylinder of variable aspect ratio ranging from 2 to 20. Their computational domain shares some similarities with the one of Inoue and Sakuragi (2008). Indeed the length and the height depend on L and equal respectively $25L$ and 12, while the depth is fixed and equals to $50D$.

After numerous calculations the size of the domain was defined using a length proportional to the equivalent spherical diameter (the diameter of a sphere with equivalent volume) : $D_e = (LD^2)^{1/3}$. This choice ensures that the domain evolves with the size of the particle while remaining relatively small. Several test cases have shown that this convention remains valid up to $L/D = 10$.

The simulations are performed in a cuboid domain on an irregular cartesian grid. Its dimension evolves with the size and angle of the particle with the inflow. Indeed the length L_x, height L_y and depth L_z of the domain are respectively $30D_e + L\cos\theta$, $20D_e + L/2\cos\theta$ and $20D_e$ (figure 1), where θ is the angle between the symmetry axis of the cylinder and the incoming flow. L_y and L_z are chosen sufficiently large to avoid wall effect in low Reynolds number flow. On the other hand L_z is defined in such a way that the wake can grow without being perturbed by the outer boundary. The domain can be divided in two main regions. An inner region around the cylinder which is made of regular cell. The dimension of this subdomain (L_{xb}, L_{yb}, L_{zb}) are specified in figure 1. L_{xb} is larger downstream of the cylinder to ensure that the near wake is well captured. The outer region is made of stretched cell which smoothly match the size of cells of the inner region.

Boundary conditions are prescribed as follow. Symmetry boundary conditions are imposed on the lateral walls : $\partial u/\partial n = 0, v = 0, w = 0$ where u, v, w are respectively the x,y and z components of the velocity vector. At the inlet a uniform velocity profile is imposed $(U,0,0)$. The imposition of the outlet boundary condition is not straightforward and different choices can be found in the literature (Prosperetti and Tryggvason, 2009, p. 36). The choice made in the PeliGRIFF code is a zero gradient condition $\partial \mathbf{u}/\partial n = 0$ which have been used with success by the past to study the unsteady force on a sphere (Kim and Elghobashi, 1998). In all computations the time step was fixed to $\Delta t = 2.5 \times 10^{-3}$ and specified in order to satisfy the CFL condition.

RESULTS

In the following subsections, the numerical method described above is applied to the study of the flow past a yawed cylinder of finite-length. Before analysing our results a mesh sensitivity analysis is performed by comparing our solutions to those of Auguste (2010). His results for a cylinder aligned with the flow direction $\theta = 0$ obtained with boundary fitted method are considered as references. The range $Re \in [25;200]$ and $Re = 360$ are analysed in detail. Then the flow past a yawed cylinder $0 \leq \theta \leq 90$ of aspect ratio 3 is studied. The Reynolds number $Re = \rho UD/\mu$ is set to 200. The choice of the lengthscale for the Reynolds numbers is far from straightforward. Indeed several conventions are used in the literature : Sears (1948) used the length of the cylinder, Vakil and Green (2009) used the diameter and Hölzer and Sommerfeld (2009) the equivalent diameter. Our choice is guided by its simplicity. The Reynolds number, the yawed angle θ and the aspect ratio L/D, fully characterized the system. The analysis to come involves other dimensionless parameters. The Strouhal $St = fD/U$ number is commonly defined when the wake and the force experienced by the body become unsteady and periodic. It compares the frequency of vortex shedding f to

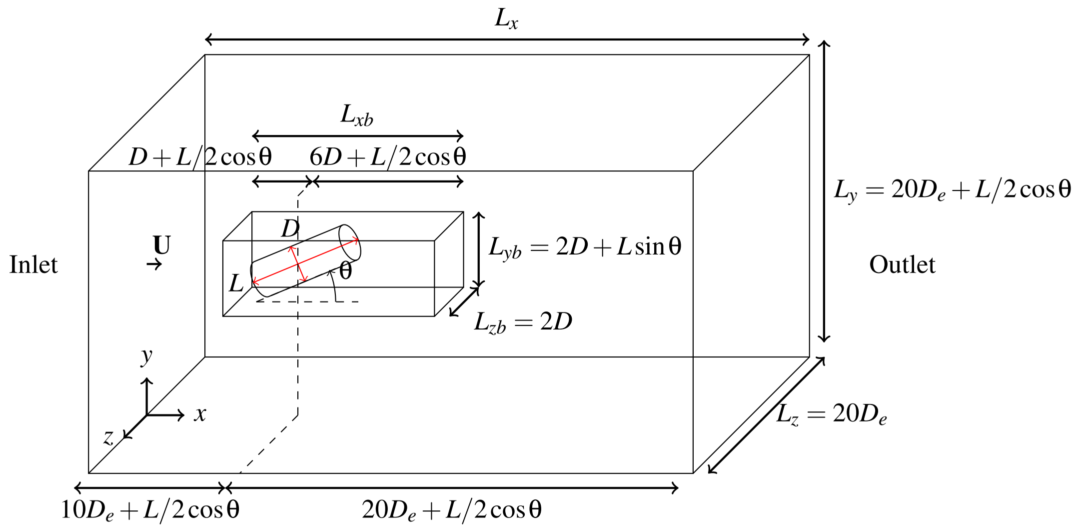

Figure 1: Scheme of the computational domain.

the characteristic frequency of the flow U/D. To describe the efforts exerted on the body the drag coefficient is defined as follow $C_D = F_x/(1/2\rho U^2 LD)$. This is the ratio between the hydrodynamic force in the streamwise direction F_x and a characteristic pressure force in inertial regime $1/2\rho U^2 LD$ where LD is proportional to the lateral area of the cylinder. It is common in practise to define the drag coefficient of a bluff body using the area of the projection of the body on a plane normal to the streamwise direction (Batchelor, 1967, p 339). Our choice to used LD as the reference area for the drag coefficient was guided by two main reasons. When $L \gg D$ and $\theta > 0$ the projected area of the disk becomes negligible compared to the lateral area of the cylinder. Moreover, since the reference area does not depend on θ, comparison between hydrodynamic efforts at different yaw angles are made simpler.

Flow past a $L/D = 1$ cylinder with $\theta = 0$

In this subsection our results are compared with those of Auguste (2010) obtained with the IMFT/JADIM code. A cylinder of aspect ratio 1 aligned in the streamwise direction is considered. Auguste (2010) identify 6 regimes depending on the Reynolds number. For $Re \lesssim 278$ the wake is stationary and axisymetric : a toroidal vortex remains downstream of the cylinder. This vortex is usually called standing eddy (Batchelor, 1967, p 330). In the range $278 \lesssim Re \lesssim 355$ the axial symmetry is lost. However the wake still maintain a plan of symmetry with two counter rotating vortices downstream of the cylinder. This regime called bifid wake is also observed for the flow past a sphere for $212 \lesssim Re \lesssim 273$ (Ern *et al.*, 2012; Ghidersa and Dusek, 2000). For higher Reynolds number ($355 \lesssim Re \lesssim 395$) the wake becomes unsteady while keeping its planar symmetry. This regime is characterized by one vortex shedding frequency. The two first bifurcations encountered with $L/D = 1$ ($\theta = 0$) are consistent with those observed for the sphere (Ern *et al.*, 2012) and for $L/D = 1/3$ ($\theta = 0$) (Auguste *et al.*, 2010). An intermediate regime arises for ($395 \lesssim Re \lesssim 420$) where a second frequency close to the third of the primary one appears. The bifurcation scenario is distinct from the one observed with $L/D = 1/3$ where the planar symmetry is lost (regime called Knit-Knot mode in Auguste *et al.* (2010)). For higher Reynolds number the planar symmetry is partially broken. The planar symmetry is fully broken for $Re = 450$ and the wake becomes fully three dimensional and chaotic. To demonstrate the ability of our approach to describe the flow past a yawed cylinder, we selected two regimes described above : the stationary regime with axial symmetry and the first unsteady regime.

		C_D	$E(C_D)\%$	l_R	$E(l_R)\%$
$Re = 25$	Auguste (2010)	9.2868	-	0.430	
	16 cells$/D$	9.4441	1.6933	0.453	5.35
	32 cells$/D$	9.3591	0.77811	0.447	3.84
$Re = 50$	Auguste (2010)	6.1591	-	0.720	-
	16 cells$/D$	6.2668	1.7486	0.741	2.99
	32 cells$/D$	6.2034	0.72013	0.732	1.67
$Re = 100$	Auguste (2010)	4.2210	-	1.12	-
	16 cells$/D$	4.3533	3.1338	1.17	4.02
	32 cells$/D$	4.2532	0.76104	1.14	1.43
$Re = 200$	Auguste (2010)	2.9468	-	1.630	-
	16 cells$/D$	3.2466	10.173	1.86	14.1
	32 cells$/D$	3.0324	2.9033	1.68	2.79

Table 1: Comparison of drag coefficient and length of standing eddy given by our numerical method and the one of (Auguste, 2010). The number of cells distributed along the cylinder diameter varies from 16 to 32. $E(C_D)$ and $E(l_R)$ represent respectively the relative error made on the drag and on the length of the standing eddy.

Table 1 shows the drag force and recirculation length for different Reynolds numbers and increasingly refined meshes. The length l_R is taken from the downstream extremity of the cylinder to the end of the eddy. This former point is fitted with a fourth-order polynomial. The error made on the drag coefficient using the coarsest grid (16 points per diameter) is less than 3.5% except for the highest Reynolds number. Since the thickness of the boundary layer scales as $O(D/Re^{1/2})$, there is approximatively one point to describe the viscous layer at $Re = 200$. This is far from being sufficient, since even for boundary fitted mesh 5 five points are necessary to accurately describe the viscous boundary layer (Auguste, 2010). The error made on l_R using the coarsest grid is large for all Reynolds number. This error decreases significantly using a grid twice more refined. However we can still note that the error made on l_R is higher than 3% for the smaller Reynolds number. The increase of numerical errors for low Reynolds number flows was pointed out by

Wachs *et al.* (2015). [1]Indeed the error made with the time splitting strategy scales as $\Delta t/Re$ (Perot, 1993).

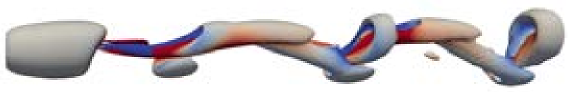

Figure 2: Wake patterns of a $L/D = 1$ cylinder aligned with the streamwise direction at $Re = 360$. 96 cells are distributed along the cylinder diameter. The wake is visualized using the Q criterion. Isosurface of $Q = 10^{-3}$ are shown. Those isosurfaces are coloured by the horizontal vorticity ranging from -0.2 to 0.2.

Figure 2 shows the vortex shedding behind a cylinder at $Re = 360$ (the wake is visualized using the Q criterion (Hunt *et al.*, 1988)). The wake keep a planar symmetry in the (x,y). Hairpin vortices are shed periodically behind the cylinder. This type of wake is a distinctive feature of wake instability since it has been observed by the past for the flow past a sphere (Sakamoto and Haniu, 1990), cylinder (Inoue and Sakuragi, 2008) and even when a sphere cross a fluid-fluid interface (Pierson and Magnaudet, 2017a). The vortex structure are double-sided that is opposite oriented hairpin vortices are shed alternatively (Inoue and Sakuragi, 2008). Moreover the hairpin vortices are not symmetric. Indeed the top vortices extend longitudinally after the hairpin loop while the bottom one not. This asymmetry of the hairpin cortices induces an averaged non-zero lift force on the body (the direction of the lift force is defined unambiguously in that case owing of the wake symmetry plane).

		C_D	$E(C_D)\%$	St	$E(St)\%$
$Re = 360$	Auguste (2010)	0.578	-	0.118	-
	16 cells$/D$	0.808	39.8	-	-
	32 cells$/D$	0.678	17.3	0.124	4.67
	64 cells$/D$	0.609	5.44	0.118	0.113
	96 cells$/D$	0.597	3.36	0.117	0.762

Table 2: Comparison of mean drag coefficient and Strouhal number given by our numerical method and the one of (Auguste, 2010). The number of cells distributed along the cylinder diameter vary from 16 to 96. $E(C_D)$ and $E(St)$ represent respectively the relative error made on the drag an on the Strouhal number.

Table 2 shows the drag coefficient and Strouhal number for increasingly refined mesh. The value of the drag coefficient given is averaged on at least 10 periods. For the coarsest grid (16 cells per diameter) the error made on the drag coefficient is closed to 40%. Moreover the wake is chaotic which prevent from defining a characteristic frequency of vortex shedding and thus the Strouhal number. The error made on the drag is less than 20% when 32 cells are distributed along the cylinder diameter. The wake (not shown here) consist of hairpin vortices which are are not shed periodically. Indeed a second frequency appears in the wake (close to the fourth of the expected one) which is a pure numerical artefact. It remains possible to define the Strouhal number based on the highest frequency: the resulting error is less than 5%. The spurious frequency disappear when using the 64 cells per diameter mesh. For that case, table 2 illustrates that the error made on C_D is more than 5% while the error made on St is less than 1%. For the more refined mesh the error on C_D is less than 3.5%.

Tables 1 and 2 point out an interesting behaviour of our fictitious domain approach. For all configuration studied the drag is always overestimated in comparison to the reference results. Numerical diffusion is a possible candidate for this overestimation. The source of this numerical error is investigated by our team. In light of those results it appears necessary to used at least 64 points per diameter to accurately describe the unsteady regime.

Flow past a yawed cylinder $L/D = 3$ cylinder

So far the present numerical method was used for comparison with existing results of the literature. We now focus on the other main motivation of this paper which is the investigation of the impact of the yawed angle on the flow structures and the efforts acting on the cylinder. The flow past a cylinder of aspect ratio three is considered. This setup is particularly relevant for chemical engineering applications since cylindrical pellets of this kind of aspect ratio are frequently used in fixed bed reactors. The Reynolds number is fixed and equals 200 which seems to be sufficiently high to see the appearance of wake instabilities (Inoue and Sakuragi, 2008). 64 cells are distributed along the diameter of the cylinder. Seven angles of inclination are studied ranging from 0° to 90° by step of 15°. The size of the resulting mesh vary from 61×10^6 cells to 91×10^6cells. For the sake of brevity we will only focus on the wake of a few configurations which show contrasted behaviour. Then we will study the force and torque experienced by the particle.

Wake patterns

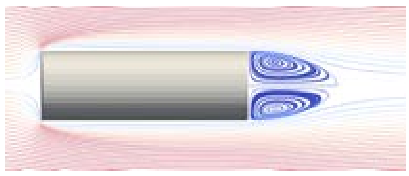

Figure 3: Standing eddy behind a $L/D = 3$ cylinder at $Re = 200$. Instantaneous streamlines on the y-z plane are coloured by the axial velocity.

Figure 3 shows the streamline patterns for $L/D = 3$, $\theta = 0$ and $Re = 200$. The wake is steady and a toroidal vortex appeared behind the cylinder. The length of the recirculation zone is $1.31D$ smaller than the one observed for $L/D = 1$ at the same Reynolds number (table 1).

Figure 4: Vortical structure for a cylinder tilted with an angle $\theta = 15°$ at $Re = 200$. Isosurface of $Q = 10^{-2}$ coloured by the longitudinal vorticity ranging from -0.2 to 0.2.

Figure 4 shows two streamwise vortices, which look like the arms of a squid, in the wake of $\theta = 15°$ cylinder. The two vortices are steady and form a counter rotating vortex pair. This regime called bifid wake for a sphere was described

[1]The increase of numerical errors for low Reynolds number flow past immersed boundaries were also observed by Kempe and Fröhlich (2012) and Pierson and Magnaudet (2017b). In their cases this was a direct consequences of the imposition of the Immersed boundary forcing before the implicit step of the Cranck-Nicholson method. This create an error on the forcing term which scales as $O(\Delta t\mu/\rho)$.

in the previous section. The bottom region of the cylinder presents a bulge made of contra-rotative vortices. The entire wake keeps a reflectional symmetry with respect to the (x,y) plane.

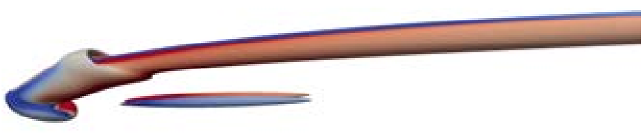

Figure 5: Vortical structure for a cylinder tilted with an angle $\theta = 30°$ at $Re = 200$. Isosurface of $Q = 10^{-3}$ coloured by the longitudinal vorticity ranging from -0.2 to 0.2.

The flow past a $\theta = 30°$ cylinder is closed to the flow past a $\theta = 15°$ cylinder even if we note the apparition of another vortex pair below the first one (figure 5). The sense of rotation of the four vortices is alternate as shown by the sense of the streamwise vorticity. This regime bears similarities with the "octopus" regime first observed by Inoue and Sakuragi (2008) for the flow past a $L/D = 1$, $\theta = 90$ cylinder at Reynolds 150. The main difference between both regimes (ours and the one of Inoue and Sakuragi (2008)) is the asymmetry between the magnitude of the two vortex pairs.

Figure 6: Vortical structure for a cylinder tilted with an angle $\theta = 75°$ at $Re = 200$. Isosurface of $Q = 10^{-2}$ coloured by the longitudinal vorticity ranging from -0.2 to 0.2.

For yawed angles larger than 60°, the wake becomes unsteady. Figure 6 shows the wake behind a $\theta = 75°$ cylinder. Hairpin vortices are shed periodically. Those vortices are double sided in the sense that vortices of opposite sense of rotation are shed. The wake seems to be symmetric with respect to the (x,z) plane but the hairpin vortices are tilted and not mutually parallel.

C_D	C_{Ly}	C_{Lz}	St_y	St
0.83	-0.16	$8.6{\times}10^{-4}$	0.056	0.126

Table 3: Drag, lift coefficients and Strouhal number for a $L/D = 3$, $\theta = 75°$ cylinder at $Re = 200$. C_D, C_{Ly} and C_{Lz} are respectively the mean drag, mean lift on y and z direction. The Strouhal numbers St_y and St are given respectively by the frequency of oscillation of C_{Ly} and the vortex shedding frequency.

Table 3 shows the drag and side force exerted on the body in the case of figure 6. The side coefficients C_{Ly} and C_{Lz} are calculated using the same convention as for C_D. The mean of C_{Ly} is non-zero which tends to confirm the absence of a reflectional symmetry plane with respect to (x,z). On the other hand C_{Lz} is really close to zero since the force oscillations along z are almost periodic. The Strouhal number St is approximatively 15% smaller than the one observed when $\theta = 90°$ (not shown here) for the same Reynolds number. Decrease of the Strouhal number when decreasing θ has been observed by the past by Ramberg (1983) for long cylinders ($L/D \geqslant 20$). The impact of the yaw angle on the vortex shedding frequency of short cylinder is let for future research. The Strouhal number St_y obtained using the frequency of force oscillations in the y direction is approximatively two times smaller than St. Two vortex are shed during one oscillation period of C_{Ly}.

For $\theta = 90°$ double-sided hairpin vortices are still observed (not shown here). Since this regime was observed by Inoue and Sakuragi (2008) until $Re = 100$ this extend the range of Reynolds number for the appearance of this regime.

Drag, lift and torque coefficients

In this section the efforts on the $L/D = 3$ yawed cylinder at $Re = 200$ are investigated. A summary of current approaches to describe the force and momentum on a yawed cylinder can be found in appendix.

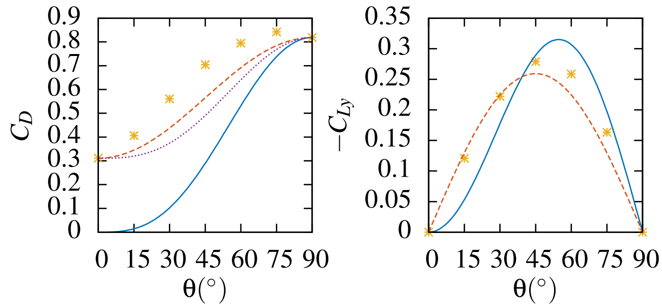

Figure 7: Drag and lift coefficient at various yaw angle. $*$: numerical results, $-$: principle of independence (equation 5 and 6), $--$: linear law (equation 3 and 4), ..: empirical relation of Rosendahl (2000) (equation 7).

The independence principle in its original form (equation 5) does not fit well with numerical results (figure 7 left) since the drag of the cylinder when $\theta = 0$ is not taken into account. When this drag is taken into account (equation 7) the agreement is better but there are still important difference in the range $30° \leq \theta \leq 60°$. For all the angles of incidence studied the linear law gives better results than the independence principle and its modification due to Rosendahl (2000).

The agreement between the independence principle and the numerical results is better for the lift force (figure 7 right). However the linear law (equation 4) is still more accurate especially for $\theta \leq 30°$. This lack of accuracy of the independence principle may be due to the fact that all computations were made with a fixed Reynolds number. The Reynolds number could be adapted in function of the yawed angle as in the numerical experiments of Vakil and Green (2009).

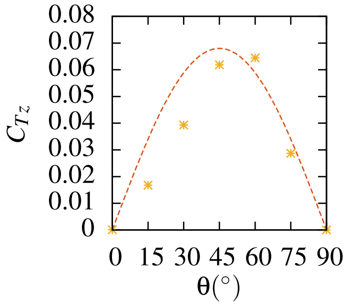

Figure 8: Torque coefficient at various yaw angle. $*$: numerical results, $--$: $C_{Tz} = 0.068\sin(2\theta)$ (appendix).

Figure 8 shows the torque coefficient $C_{Tz} =$

$T_z/(1/2\rho U^2 L^2 D)$ where T_z is the hydrodynamic torque along the z direction, for various angles of inclination. The numerical results are compared to an analytical law obtained in the Oseen regime (Khayat and Cox) : $C_{Tz} = C_{Tz\theta=45^\circ}\sin(2\theta)$ where $C_{Tz\theta=45^\circ}$ is a coefficient fitted to the the numerical results. The torque are zero for $\theta = 0^\circ$ and $\theta = 90^\circ$, but Khayat and Cox explained that the only stable configuration is $\theta = 90^\circ$. The agreement between the numerical results and the law of Khayat and Cox is pretty good even if the numerical results curve is staggered in the high θ direction. Therefore the maximal torque is obtained for $\theta \geq 45^\circ$.

CONCLUSION

The aim of this work was to demonstrate the ability of a fictitious domain method to accurately simulate the flow past a finite-end cylinder tilted to the flow. The flow past a $L/D = 1$ cylinder aligned with the flow direction was computed and compared with the results of Auguste (2010) who used a boundary-fitted method. The obtained results compares favourably with the one of Auguste (2010) when 32 points per diameter are distributed along the cylinder diameter in steady flow and 64 points in unsteady flow.

The present approach was then applied to the flow past a $L/D = 3$ yawed cylinder at $Re = 200$. Three different regimes were observed depending on the yaw angle θ. For $\theta = 0^\circ$ the wake pattern behind the body is a steady axisymmetric toroidal vortex. A first bifurcation is observed in the range $0^\circ \leq \theta \leq 15^\circ$: the wake breaks the axisymmetry but retains a reflectional symmetry with respect to the (x, y) plane. This regime is characterized by two steady counter-rotating vortices. Two other counter-rotating vortices appears below the first one for $\theta = 30^\circ$. The wake becomes unsteady for $\theta \leq 60^\circ$. The plane of symmetry is partially broken and double-sided hairpin vortices are shed alternatively. The independence principle was shown to be poorly accurate to describe the drag force on a yawed cylinder. For the aspect ratio and Reynolds number studied the linear law given by the Stokes regime seems to be better suited. Thus the range of validity of the independence principle (in terms of Reynolds number and aspect ratio) must be investigated deeper. Indeed it gives very accurate results for yawed cylinder of infinite length at high Reynolds number (Zhao *et al.*, 2009).

Despite the good agreement between our results and the one of Auguste (2010) several points need to be clarified. First the effect of the numerical scheme used to discretize the convective term of the momentum equation have to be investigated. This may give some hints for the source of numerical diffusion observed in the second section. Secondly several tests have to be perform for the case $L/D = 3$, $Re = 200$ $\theta = 75^\circ$ in order to investigate if the oscillations of the side force along y are numerical errors or not.

Finally it would be interesting to study the flow past cylinder aligned with the flow, in order to obtain a lower bound for the drag on the same cylinder tilted with the flow. Several points may be investigated. Batchelor (1967, p. 337) pointed out that the boundary layer detachment occurs when the body is not sufficiently slender. It would be interesting to quantify the impact of L/D over the apparition of the standing eddy. On the other hand Ern *et al.* (2012) gave a threshold value for the Reynolds number associated with the first bifurcation of a disk ($L/D \leq 1$). It is estimated as $Re_c = 116.5(1 + L/D)$. The investigation of the validity of this law for $L/D \geq 1$ constitute a promising task.

ACKNOWLEDGEMENTS

This work was granted access to the HPC resources of CINES under the allocation c20162a7728.

REFERENCES

ARDEKANI, M.N., COSTA, P., BREUGEM, W.P. and BRANDT, L. (2016). "Numerical study of the sedimentation of spheroidal particles". *International Journal of Multiphase Flow*, **87**, 16–34.

AUGUSTE, F. (2010). "Instabilités de sillage générées derrière un corps solide cylindrique, fixe ou mobile dans un fluide visqueux". *These de doctorat*.

AUGUSTE, F., FABRE, D. and MAGNAUDET, J. (2010). "Bifurcations in the wake of a thick circular disk". *Theoretical and Computational Fluid Dynamics*, **24(1)**, 305–313.

BATCHELOR, G.K. (1967). *An introduction to fluid dynamics*. Cambridge university press.

BERNARD, M., CLIMENT, E. and WACHS, A. (2016). "Controlling the quality of two-way euler/lagrange numerical modeling of bubbling and spouted fluidized beds dynamics". *Industrial & Engineering Chemistry Research*.

BIGOT, B., BONOMETTI, T., LACAZE, L. and THUAL, O. (2014). "A simple immersed-boundary method for solid–fluid interaction in constant-and stratified-density flows". *Computers & Fluids*, **97**, 126–142.

CAPECELATRO, J. and DESJARDINS, O. (2013). "An euler–lagrange strategy for simulating particle-laden flows". *Journal of Computational Physics*, **238**, 1–31.

CHRUST, M., BOUCHET, G. and DUŠEK, J. (2010). "Parametric study of the transition in the wake of oblate spheroids and flat cylinders". *Journal of Fluid Mechanics*, **665**, 199–208.

DORAI, F., TEIXEIRA, C.M., ROLLAND, M., CLIMENT, E., MARCOUX, M. and WACHS, A. (2015). "Fully resolved simulations of the flow through a packed bed of cylinders: Effect of size distribution". *Chemical Engineering Science*, **129**, 180–192.

ERN, P., RISSO, F., FABRE, D. and MAGNAUDET, J. (2012). "Wake-induced oscillatory paths of bodies freely rising or falling in fluids". *Annual Review of Fluid Mechanics*, **44**, 97–121.

GHIDERSA, B. and DUSEK, J. (2000). "Breaking of axisymmetry and onset of unsteadiness in the wake of a sphere". *Journal of Fluid Mechanics*, **423**, 33–69.

HOERNER, S.F. (1965). *Fluid-dynamic drag: practical information on aerodynamic drag and hydrodynamic resistance*. Hoerner Fluid Dynamics Midland Park, NJ.

HÖLZER, A. and SOMMERFELD, M. (2008). "New simple correlation formula for the drag coefficient of non-spherical particles". *Powder Technology*, **184(3)**, 361–365.

HÖLZER, A. and SOMMERFELD, M. (2009). "Lattice boltzmann simulations to determine drag, lift and torque acting on non-spherical particles". *Computers & Fluids*, **38(3)**, 572–589.

HU, H.H., JOSEPH, D.D. and CROCHET, M.J. (1992). "Direct simulation of fluid particle motions". *Theoretical and Computational Fluid Dynamics*, **3**, 285–306.

HUNT, J.C., WRAY, A.A. and MOIN, P. (1988). "Eddies, streams, and convergence zones in turbulent flows".

INOUE, O. and SAKURAGI, A. (2008). "Vortex shedding from a circular cylinder of finite length at low reynolds numbers". *Physics of Fluids*, **20(3)**, 033601.

JACKSON, R. (2000). *The dynamics of fluidized particles*. Cambridge University Press.

KEMPE, T. and FRÖHLICH, J. (2012). "An improved immersed boundary method with direct forcing for the simulation of particle laden flows". *Journal of Computational Physics*, **231(9)**, 3663–3684.

KHAYAT, R. and COX, R. (). "Inertia effects on the motion of long slender bodies". *Journal of Fluid Mechanics*, **209**.

KIM, I. and ELGHOBASHI, S. (1998). "On the equation for spherical-particle motion: effect of reynolds and acceleration numbers". *Journal of Fluid Mechanics*, **367(1)**, 221–253.

MITTAL, R. and IACCARINO, G. (2005). "Immersed boundary methods". *Annu. Rev. Fluid Mech.*, **37**, 239–261.

PEROT, J.B. (1993). "An analysis of the fractional step method". *Journal of Computational Physics*, **108(1)**, 51–58.

PIERSON, J.L. and MAGNAUDET, J. (2017a). "Inertial settling of a sphere through an interface. part 1: From sphere flotation to wake fragmentation". *J. Fluid Mech (submitted).*

PIERSON, J.L. and MAGNAUDET, J. (2017b). "Inertial settling of a sphere through an interface. part 2: Sphere and tail dynamics". *J. Fluid Mech (submitted).*

PIERSON, J.L., HAMMOUTI, A., AUGUSTE, F. and WACHS, A. (2017). "Direct numerical simulation of the flow past a finite-end yawed cylinder : a fictitious domain approach". *(in preparation).*

PROSPERETTI, A. and TRYGGVASON, G. (2009). *Computational methods for multiphase flow*. Cambridge university press.

RAHMANI, M. and WACHS, A. (2014). "Free falling and rising of spherical and angular particles". *Physics of Fluids*, **26(8)**, 083301.

RAMBERG, S. (1983). "The effects of yaw and finite length upon the vortex wakes of stationary and vibrating circular cylinders". *Journal of Fluid Mechanics*, **128**, 81–107.

ROSENDAHL, L. (2000). "Using a multi-parameter particle shape description to predict the motion of non-spherical particle shapes in swirling flow". *Applied Mathematical Modelling*, **24(1)**, 11–25.

SAKAMOTO, H. and HANIU, H. (1990). "A study on vortex shedding from spheres in a uniform flow". *ASME, Transactions, Journal of Fluids Engineering*, **112**, 386–392.

SEARS, W.R. (1948). "The boundary layer of yawed cylinders". *Journal of the aeronautical sciences*.

UHLMANN, M. (2005). "An immersed boundary method with direct forcing for the simulation of particulate flows". *Journal of Computational Physics*, **209**, 448 – 476.

UHLMANN, M. and DUŠEK, J. (2014). "The motion of a single heavy sphere in ambient fluid: a benchmark for interface-resolved particulate flow simulations with significant relative velocities". *International Journal of Multiphase Flow*, **59**, 221–243.

VAKIL, A. and GREEN, S.I. (2009). "Drag and lift coefficients of inclined finite circular cylinders at moderate reynolds numbers". *Computers & Fluids*, **38(9)**, 1771–1781.

WACHS, A. (2009). "A dem-dlm/fd method for direct numerical simulation of particulate flows: Sedimentation of polygonal isometric particles in a newtonian fluid with collisions". *Computers & Fluids*, **38(8)**, 1608–1628.

WACHS, A., HAMMOUTI, A., VINAY, G. and RAHMANI, M. (2015). "Accuracy of finite volume/staggered grid distributed lagrange multiplier/fictitious domain simulations of particulate flows". *Computers & Fluids*, **115**, 154–172.

WIESELSBERGER, C. (1922). "Further data on the law of liquid and air drag". *Phys. Z*, **23**, 219–224.

ZDRAVKOVICH, M., BRAND, V., MATHEW, G. and WESTON, A. (1989). "Flow past short circular cylinders with two free ends". *Journal of fluid mechanics*, **203**, 557–575.

ZDRAVKOVICH, M.M. (1997). *Flow around Circular Cylinders: Volume 1: Fundamentals*, vol. 1. Oxford university press.

ZDRAVKOVICH, M.M. (2003). *Flow around Circular Cylinders: Volume 2: Applications*, vol. 2. Oxford university press.

ZHAO, M., CHENG, L. and ZHOU, T. (2009). "Direct numerical simulation of three-dimensional flow past a yawed circular cylinder of infinite length". *Journal of Fluids and Structures*, **25(5)**, 831–847.

APPENDIX : EFFORTS ON A YAWED CYLINDER

The force and torque experienced by a finite cylinder in a stationary flow are not known exactly even in the Stokes flow regime. However in this regime owing to the linearity of the equations, the force on a cylinder tilted with an angle θ (figure 1) can be related to the force on the same object tilted with angles $\theta = 0$ and $\theta = 90$ as :

$$C_D = C_{D\theta=0^\circ} \cos^2(\theta) + C_{D\theta=90^\circ} \sin^2(\theta) \quad (3)$$

$$C_{Ly} = C_{Dy\theta=0^\circ} \cos(\theta)\sin(\theta) - C_{Dy\theta=90^\circ} \sin(\theta)\cos(\theta) \quad (4)$$

In the Stokes flow regime, the torque on a cylinder is $\mathbf{0}$. A cylinder will keep its initial orientation while falling under gravity. This specific property is lost when including weak effect of inertia (Khayat and Cox). When $Re \ll 1$ the torque along z evolves as $T_z \propto \sin(2\theta)$.

For high Reynolds numbers there is another interesting theory which relates the force on a yawed cylinder to the force on the same cylinder perpendicular to the flow. Indeed the independence principle states that the normal force on an infinitely long yawed cylinder in a a flow of velocity U is the same that the one exerted upon the same cylinder placed in a cross flow of velocity $U\sin(\theta)$ (Sears, 1948). The drag and lift coefficients can be written as (Hoerner, 1965) :

$$C_D = C_{D\theta=90^\circ} \sin^3(\theta) \quad (5)$$

$$C_{Ly} = C_{Dy\theta=90^\circ} \sin^2(\theta)\cos(\theta) \quad (6)$$

In order to take into account into the drag the force experienced by a cylinder aligned with the flow direction Rosendahl (2000) proposed the empirical relation :

$$C_D = C_{D\theta=0^\circ} + (C_{D\theta=90^\circ} - C_{D\theta=0^\circ}) \sin^3(\theta) \quad (7)$$

There are several other empirical and semi-empirical laws derived for the drag on non spherical-particles including the one of (Hölzer and Sommerfeld, 2008). Instead of using explicitly the orientation of the particle, they proposed to use the lengthwise and crosswise sphericity (whose definition can be found in their article). Their correlation give excellent agreement with existing results in the literature.